

Research

# Spectral Mismatch Correction and Spectrometric Characterization of Monolithic III–V Multi-junction Solar Cells

M. Meusel<sup>1,\*†</sup>, R. Adelhelm<sup>2</sup>, F. Dimroth<sup>1</sup>, A. W. Bett<sup>1</sup> and W. Warta<sup>1</sup>

<sup>1</sup>Fraunhofer Institute for Solar Energy Systems, Heidenhofstrasse 2, 79110 Freiburg, Germany

<sup>2</sup>Current address: Astrium GmbH, 81663 Munich, Germany

*III–V monolithic multi-junction (MJ) solar cells reach efficiencies exceeding 30% (AM1.5 global) and have applications in space and in terrestrial concentrator systems. The subcells of monolithic MJ cells are not accessible separately, which presents a challenge to measurement systems and procedures. A mathematical approach is presented which enables a fast way of spectral mismatch correction for MJ cells, thereby significantly reducing the time required for calibration. Moreover, a systematic investigation of the I–V parameters of a MJ solar cell with variation of the incident spectrum is possible, herein called ‘spectrometric characterization’. This analysis method visualizes the effects of current limitation and shifting of the operating voltage, and yields precise information about the current-matching of the subcells. MJ cells can hereby be compared without the need to match the current of the structures to a reference spectrum in advance. Further applications of the spectrometric characterization are suggested, such as for the determination of the radiation response of the subcells of MJ space solar cells or for the prediction of the annual power output of terrestrial MJ concentrator cells. Copyright © 2002 John Wiley & Sons, Ltd.*

## INTRODUCTION

III–V multi-junction (MJ) solar cells, for example the monolithic  $\text{Ga}_{0.51}\text{In}_{0.49}\text{P}/\text{GaAs}$  dual-junction cell, reach efficiencies exceeding 30% (AM1.5 global)<sup>1</sup> by using different bandgaps in order to reduce the losses due to thermal relaxation. Their applications exist in space and in terrestrial concentrator systems. In general, MJ solar cells can consist either of separate cells mechanically stacked on top of each other, or of monolithically integrated cells epitaxially grown on one substrate. In the latter case the subcells are interconnected in series by tunnel diodes, leading to a standard two-terminal contact (Figure 1). Thus, the subcells are not accessible separately, which poses a challenge to measurement systems and procedures for the determination of the spectral response, the *I–V* characteristics and efficiency.

\*Correspondence to: Matthias Meusel, Fraunhofer Institute for Solar Energy Systems, Heidenhofstrasse 2, 79110 Freiburg, Germany.

†E-mail: meusel@ise.fhg.de

Contract/grant sponsor: German Ministry of Economy and Technology.

Contract/grant number: 0328554E.

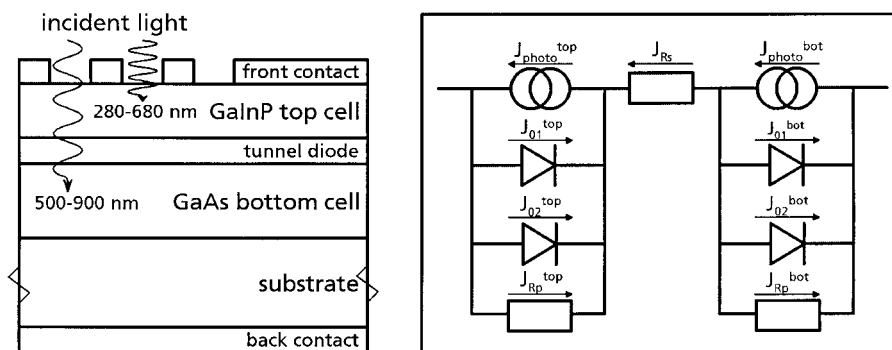


Figure 1. Basic structure, functionality and equivalent circuit of a monolithic GaInP/GaAs dual-junction cell

The most important effect observed when measuring monolithic MJ solar cells is the current limitation. The short-circuit current of the MJ cell is in general equal to the minimum of the photocurrents of the subcells. Exceptions to this rule occur, when the subcell with the lowest photocurrent has a low shunt resistance or a low reverse breakdown voltage. Changing the incident spectrum causes a shift of the operating voltage of the individual subcells. The subcells with excess photocurrent can discharge only part of their photocurrent and are therefore operating at a voltage close to their open-circuit voltage. If for example the external voltage of a MJ cell is zero, the current-limiting subcell will operate at a voltage approximately equal to the sum of the negative open-circuit voltages of the other subcells. The characteristics of MJ cells are therefore very sensitive to the distribution of the incident spectrum. Especially, the fill factor was observed to vary under different spectral conditions.<sup>2,3</sup>

Thus, for the calibration of a MJ solar cell, special attention has to be given to the spectral distribution of the solar simulator. Multi-source<sup>4,5</sup> or spectrally adjustable solar simulators<sup>6,7</sup> are used to match the simulator spectrum for each subcell. In doing so, the problem arises that present measurement procedures for setting the simulator spectrum, involving the calculation of the mismatch factor<sup>8</sup> for each subcell, are very time consuming.

In this paper a faster way of spectral correction for MJ cells is presented using a multi-source simulator set-up. This method not only allows a faster calibration, but also enables a systematic investigation of the behavior of the  $I$ - $V$  parameters of a MJ solar cell to variation of the incident spectrum, hereinafter called 'spectrometric characterization'. The basic approach of spectrometric characterization has already been published<sup>9</sup> with measurement examples on amorphous silicon dual-junction solar cells. Since then procedures have been significantly improved and successfully applied to different types of III-V MJ solar cells. The intention of this paper is to motivate and to explain the measurement procedures in order to allow a deeper insight and understanding of this characterization method. To demonstrate the capabilities of spectrometric characterization, various possibilities for its application will be addressed, such as the determination of the radiation response of the subcells of MJ space solar cells, or the prediction of the annual power output of terrestrial MJ concentrator cells.

## CALIBRATION AND SPECTRAL MISMATCH CORRECTION

For the calibration of a MJ solar cell for a reference spectrum, the simulator spectrum has to be adjusted, such that each subcell generates the photocurrent that would be expected under the reference spectrum. This can be obtained by a mathematical procedure called spectral mismatch correction, which requires knowledge of the relative simulator spectrum and the relative spectral response of each individual subcell.

For the measurement of the spectral response of a subcell the effect of current limitation is utilized. The spectrum of the bias irradiation is adjusted until the subcell to be measured is limiting the current of the MJ cell. In addition, voltage biasing has to be applied for an absolute spectral measurement<sup>10</sup> because of the shift of the operating voltage of the limiting subcell. Moreover, it is useful to routinely apply voltage biasing in order to

avoid problems due to a low shunt resistance<sup>11</sup> or due to a low reverse breakdown voltage of the subcell to be measured, as observed for the low bandgap Ge cell of a GaInP/GaAs/Ge triple-junction solar cell.<sup>12</sup>

For the spectral mismatch correction a generalization of single-junction measurement procedures is used,<sup>8</sup> involving the calculation of a spectral mismatch factor  $M$ . In the case of single-junction cells, the intensity of the simulator spectrum is adjusted, until the current of the reference cell under the simulator spectrum is equal to its current under the reference spectrum divided by the mismatch factor  $M$ . If this method is applied to MJ cells, the simulator spectrum has to be adjusted in respect to the mismatch factor  $M_j$  for each subcell. This necessitates changing not only the intensity, but also the spectral distribution of the simulator, which in turn changes the values for the mismatch factors  $M_j$ . Therefore, an iterative procedure has to be applied, consisting of the measurement of the simulator spectrum, the calculation of the mismatch factor  $M_j$  for each subcell, adjusting the simulator spectrum, remeasuring the spectrum etc.<sup>13,14</sup>

In the following, a faster method for spectral correction is presented, which assumes a multi-source simulator set-up with independent light sources, the intensities of which can be adjusted without changing their spectral distribution. The geometric set-up and examples of the different spectra of the multi-source simulator of ISE CalLab are shown in Figure 2.

At first, the mathematical procedure will be derived in respect of dual-junction solar cells, for simplicity. Generalized equations for MJ cells with  $n$  junctions are given afterwards. The subscript top refers to the top and the subscript bot to the bottom subcell. The photocurrent densities  $J$  of the two subcells of a dual-junction test cell under a desired reference spectrum  $E_{\text{ref}}(\lambda)$  can be calculated by:

$$J_{\text{top}}^{\text{ref}} = \int S_{\text{top}}(\lambda) E_{\text{ref}}(\lambda) d\lambda = C_{\text{top}} \int s_{\text{top}}(\lambda) E_{\text{ref}}(\lambda) d\lambda \quad (1)$$

$$J_{\text{bot}}^{\text{ref}} = \int S_{\text{bot}}(\lambda) E_{\text{ref}}(\lambda) d\lambda = C_{\text{bot}} \int s_{\text{bot}}(\lambda) E_{\text{ref}}(\lambda) d\lambda \quad (2)$$

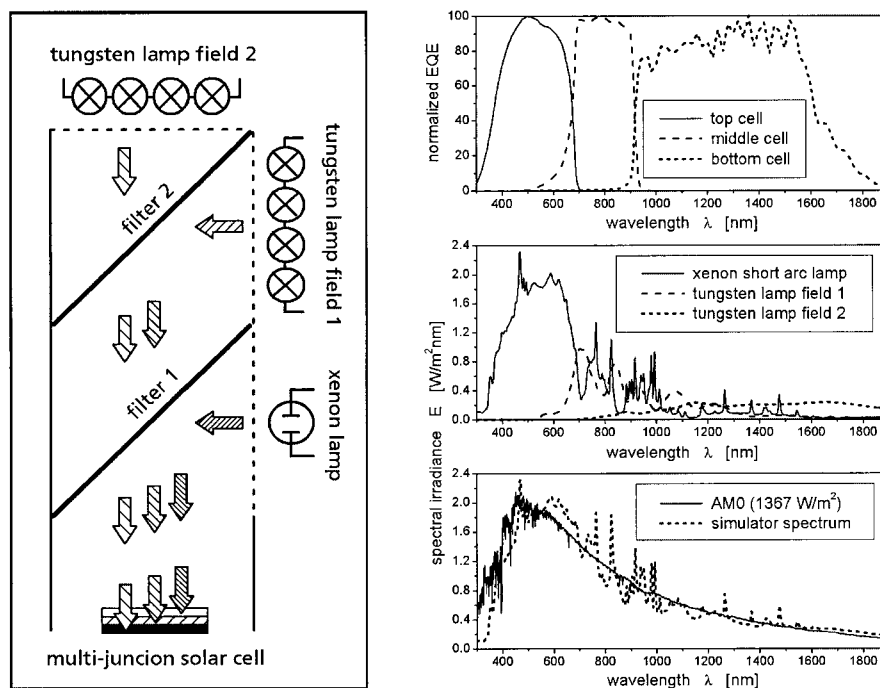


Figure 2. Schematic of the multi-source simulator at ISE CalLab (left) and spectra of the individual light sources (middle right), as used for the calibration of a Ga<sub>0.51</sub>In<sub>0.49</sub>P/Ga<sub>0.95</sub>In<sub>0.05</sub>As/Ge triple cell, of which the external quantum efficiency (EQE) is shown (top right). The total simulator spectrum (bottom right) fulfils the requirements of a class A solar simulator (IEC 904–9) with respect to the extraterrestrial sun spectrum AM0 in the range 400–1700 nm

where:  $S_{\text{top/bot}}(\lambda)$  = absolute spectral response of the top/bottom cell;  $s_{\text{top/bot}}(\lambda)$  = relative spectral response of the top/bottom cell; and  $C_{\text{top/bot}} = S_{\text{top/bot}}(\lambda)/s_{\text{top/bot}}(\lambda)$  = ratio of absolute to relative spectral response.

It has to be mentioned that, in general, only the smaller of both photocurrents will flow, due to the series connection of the subcells. The calculated photocurrents must therefore be interpreted as a generation of charge carriers instead of an external current. The photocurrent densities  $J$  of the two subcells during the measurement under a solar simulator with two independent light sources, with relative spectra given by  $e_1(\lambda)$  and  $e_2(\lambda)$ , are:

$$J_{\text{top}}^{\text{sim}} = C_{\text{top}} A_1 \int s_{\text{top}}(\lambda) e_1(\lambda) d\lambda + C_{\text{top}} A_2 \int s_{\text{top}}(\lambda) e_2(\lambda) d\lambda \quad (3)$$

$$J_{\text{bot}}^{\text{sim}} = C_{\text{bot}} A_1 \int s_{\text{bot}}(\lambda) e_1(\lambda) d\lambda + C_{\text{bot}} A_2 \int s_{\text{bot}}(\lambda) e_2(\lambda) d\lambda \quad (4)$$

where  $A_1$  and  $A_2$  are parameters by which the intensity of light sources 1 and 2 is adjusted.

For the calibration, the current generation under the simulator spectrum has to be equal to the generation under the reference spectrum for each subcell. Therefore Equations (1) and (3) as well as Equations (2) and (4) are set equal, so that  $C_{\text{top}}$  and  $C_{\text{bot}}$  cancel out:

$$A_1 \int s_{\text{top}}(\lambda) e_1(\lambda) d\lambda + A_2 \int s_{\text{top}}(\lambda) e_2(\lambda) d\lambda = \int s_{\text{top}}(\lambda) E_{\text{ref}}(\lambda) d\lambda \quad (5)$$

$$A_1 \int s_{\text{bot}}(\lambda) e_1(\lambda) d\lambda + A_2 \int s_{\text{bot}}(\lambda) e_2(\lambda) d\lambda = \int s_{\text{bot}}(\lambda) E_{\text{ref}}(\lambda) d\lambda \quad (6)$$

Equations (5) and (6) represent a two-dimensional, inhomogeneous linear equation system with two unknowns  $A_1$  and  $A_2$ , which can easily be solved by linear algebra. To ensure positive solutions only, the light sources have to be chosen such that the current generation in each subcell is mainly caused by one of the light sources (see Figure 2). The adjustment parameters  $A_1$  and  $A_2$ , multiplied by the relative spectra  $e_1(\lambda)$  and  $e_2(\lambda)$ , yield the absolute spectra  $E_1(\lambda)$  and  $E_2(\lambda)$  of the two simulator sources. The short-circuit current density generated by these spectra in a single-junction reference cell with the absolute spectral response  $S_{\text{RC}}(\lambda)$  is:

$$J_{\text{RC}}^{E_1} = A_1 \int S_{\text{RC}}(\lambda) e_1(\lambda) d\lambda \quad (7)$$

and

$$J_{\text{RC}}^{E_2} = A_2 \int S_{\text{RC}}(\lambda) e_2(\lambda) d\lambda \quad (8)$$

The solar simulator is therefore set by adjusting the intensity of the two sources, until the short-circuit current density of the reference cell satisfies Equations (7) and (8). When using only one reference cell, it must be ensured that the range of spectral sensitivity of the reference cell includes the range of sensitivity of each subcell. In regard to the measurement uncertainty, it is beneficial to use spectrally matched reference cells, analogous to the procedures involving the mismatch factor.<sup>15</sup>

A generalized version of the linear equation system (5,6) for  $n$  junctions is given by the  $n$  equations for each subcell  $j \in \{\text{top}, \dots, \text{bot}\}$ :

$$\sum_{k=1}^n A_k \int s_j(\lambda) e_k(\lambda) d\lambda = \int s_j(\lambda) E_{\text{ref}}(\lambda) d\lambda \quad (9)$$

In Equation (9)  $k$  is the index for each simulator source, ranging from 1 to  $n$ , since there are as many different light sources needed as there are subcells in the MJ cell. The generalized version of Equations (7) and (8) is given by the  $n$  equations for each simulator source  $k$ :

$$J_{\text{RC}}^{E_k} = A_k \int S_{\text{RC}}(\lambda) e_k(\lambda) d\lambda \quad (10)$$

Similar to the calculation of the mismatch factor,<sup>8</sup> the procedure shown requires the relative spectral irradiances of the simulator light sources, the relative spectral response of each junction of the test cell and the absolute spectral response of the reference cell. Comparison of measurements<sup>14</sup> with the National Renewable Energy Laboratory (NREL) in Golden, Colorado, where spectral correction is performed via the mismatch factor, showed very good agreement. The presented procedure calculates the simulator spectrum as the additive mixture of the simulator sources, which have a fixed spectral distribution  $e_k(\lambda)$ . This removes the need to remeasure the simulator spectrum, and thus the iterative procedure can be avoided.

## SPECTRAL METRIC AND SPECTROMETRIC CHARACTERIZATION

In the previous section, a mathematical procedure was presented, which enables a fast adjustment of the spectrum of a multi-source solar simulator to spectrally match a reference spectrum in regard to a specific MJ test cell. The same procedure can also be applied for other than the standard spectra AM0, AM1.5 global or direct. The behavior of a MJ cell under different spectral conditions can thus be investigated quickly. A mathematical formalism, herein after called 'spectral metric',<sup>9,16</sup> is introduced, in order to define scalar quantities, by which a spectrum can be specified. In the 'spectrometric characterization', the  $I$ - $V$  parameters of the MJ cell are recorded and plotted against these scalar quantities.

The spectral metric for a MJ solar cell constitutes an analogy to colorimetry. Since the middle of the 19th century it has been known that each color can be created by the additive mixture of three primary light sources, as for example red, green and blue light. A color can therefore be specified by three numbers,  $X$ ,  $Y$ ,  $Z$ , known as the tristimulus values, each representing the amount of one of the primary stimuli. The tristimulus values of the spectrum colors,  $\bar{x}(\lambda)$ ,  $\bar{y}(\lambda)$ ,  $\bar{z}(\lambda)$ , which show the characteristics of a spectral response curve, were determined by experiments employing a number of carefully selected observers. The tristimulus values,  $X$ ,  $Y$  and  $Z$ , of a spectrum  $E(\lambda)$  can be calculated by multiplication with  $\bar{x}(\lambda)$ ,  $\bar{y}(\lambda)$ ,  $\bar{z}(\lambda)$  for each wavelength  $\lambda$ , followed by an integration over  $\lambda$ . The chromaticity is described by the trichromatic coefficients,  $x$ ,  $y$  and  $z$ , where  $x = X/(X + Y + Z)$  etc. Because of the normalization condition,  $x + y + z = 1$ , a chromaticity can be specified by a point in the  $x$ - $y$  plane.<sup>17</sup>

In the spectral metric of a dual-junction solar cell, the 'effective' or 'actinic' irradiances  $G_{\text{eff}}^{\text{top}}$  and  $G_{\text{eff}}^{\text{bot}}$  of a spectrum  $E(\lambda)$  on the two subcells are used as measures, comparable to the tristimulus values  $X$ ,  $Y$ , and  $Z$  in colorimetry.

$$G_{\text{eff}}^{\text{top}}(E(\lambda)) = N \int S_{\text{top}}(\lambda) E(\lambda) d\lambda \quad (11)$$

$$G_{\text{eff}}^{\text{bot}}(E(\lambda)) = N \int S_{\text{bot}}(\lambda) E(\lambda) d\lambda \quad (12)$$

The effective irradiance is equal to the photocurrent density, except for a proportionality factor  $N$ , which is used for normalization and conversion to the desired units, for example  $\text{W}/\text{m}^2$ . The multi-dimensional space of all spectra is therefore mapped on the two-dimensional vector space of positive real numbers, such that each spectrum  $E(\lambda)$  can be represented by a point  $(G_{\text{eff}}^{\text{top}}, G_{\text{eff}}^{\text{bot}}) \in \mathbb{R}_+^2$ . Comparable to the chromaticity, the current mismatch depends only on the effective irradiance coefficients  $G_{\text{eff}}^{\text{top}}/(G_{\text{eff}}^{\text{top}} + G_{\text{eff}}^{\text{bot}})$  and  $G_{\text{eff}}^{\text{bot}}/(G_{\text{eff}}^{\text{top}} + G_{\text{eff}}^{\text{bot}})$ . Owing to the normalization condition, that the sum of the effective irradiances coefficients is equal to one, the dimensionality of the problem can be reduced. Each spectrum can be ascribed a current mismatch by a point on a line.

In general, there are several ways of choosing spectra for the investigation.<sup>18</sup> One approach is to vary the simulator spectrum in relation to a reference spectrum. We will therefore postulate that the sum of the effective irradiances on all subcells of the spectra used for the investigation is equal to that of a specific reference spectrum:

$$G_{\text{eff}}^{\text{top}}(E(\lambda)) + G_{\text{eff}}^{\text{bot}}(E(\lambda)) = G_{\text{eff}}^{\text{top}}(E_{\text{ref}}(\lambda)) + G_{\text{eff}}^{\text{bot}}(E_{\text{ref}}(\lambda)) = \text{const} \quad (13)$$

Equation (13) defines a line of spectra in the two-dimensional space of the spectral metric, for which the photocurrent of the individual subcells varies, while their sum is constant. This corresponds to a changing of the photocurrent of the subcells by varying the design of the MJ cell instead of irradiating different spectra. If for example the top cell base layer is thinned, more photons are transmitted to the bottom cell, leading to an increase of its photocurrent, while the photocurrent of the top cell decreases. However, the sum of the photocurrents of both subcells stays approximately the same.

For the formalism described above, the absolute spectral responses  $S_{\text{top}}(\lambda)$  and  $S_{\text{bot}}(\lambda)$  were used (Equations 11, 12). However, it is desirable to have a procedure that requires only the relative spectral responses in order to avoid the additional uncertainty of absolute measurements. Therefore, the following equation is used, which is equivalent to Equation (13) if the photocurrents of the subcells are equal under the reference spectrum.

$$\frac{G_{\text{eff}}^{\text{top}}(E(\lambda))}{G_{\text{eff}}^{\text{top}}(E_{\text{ref}}(\lambda))} + \frac{G_{\text{eff}}^{\text{bot}}(E(\lambda))}{G_{\text{eff}}^{\text{bot}}(E_{\text{ref}}(\lambda))} = \frac{\int S_{\text{top}}(\lambda)E(\lambda)d\lambda}{\int S_{\text{top}}(\lambda)E_{\text{ref}}(\lambda)d\lambda} + \frac{\int S_{\text{bot}}(\lambda)E(\lambda)d\lambda}{\int S_{\text{bot}}(\lambda)E_{\text{ref}}(\lambda)d\lambda} = 2 \quad (14)$$

Equation (14) defines a line, hereafter called the ‘line of measurement’ (Figure 3), which can be interpreted as an approximation of the ‘ideal line’ defined by Equation (13). However, the line of measurement is well defined

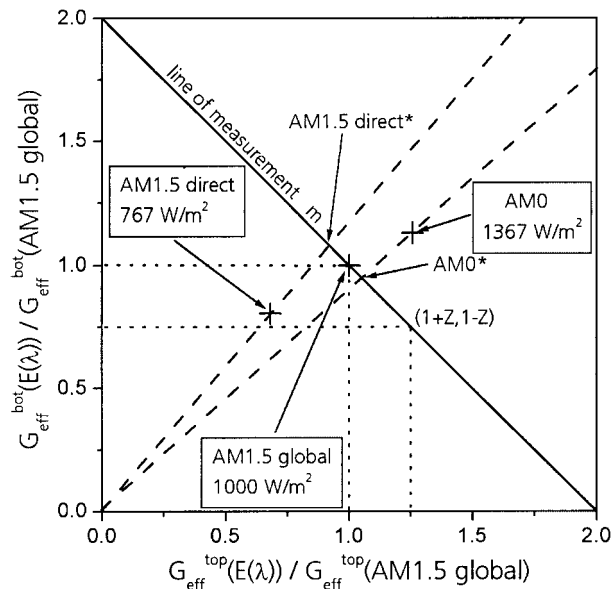


Figure 3. Standard spectra and the line of measurement  $m$  in the spectral metric of a  $\text{Ga}_{0.51}\text{In}_{0.49}\text{P}/\text{Ga}_{0.95}\text{In}_{0.05}\text{As}$  dual-junction solar cell. The effective irradiance is normalized by the effective irradiance of the reference spectrum (here AM1.5 global). Therefore, the units on the scales indicate the effective irradiance in ‘suns’. Points on the line of measurement  $m$  can be specified by the parameter  $Z$ , such that  $(1+Z, 1-Z)$  represents a spectrum, for which the photocurrent of the top cell is  $Z \cdot 100\%$  higher and the photocurrent of the bottom cell is  $Z \cdot 100\%$  smaller than under the reference spectrum. Spectra with the same relative distribution, but different total irradiance, are located along a line through the origin. Spectra with equal distribution as AM0 or AM1.5 direct can be found on the line of measurement at the intersection points AM0\* and AM1.5 direct\*

and totally sufficient for the investigation and the interpretation of the results. Only with regard to the comparison of different MJ cells might it be advantageous to correct the measured values on the line of measurement to those on the ideal line. This can be performed because the photocurrents and the effective irradiances on both subcells are known after spectrometric characterization, as will be shown later. The correction factor  $c_{\text{corr}}$  for the irradiance at the point  $(1 + Z, 1 - Z)$  is given by  $c_{\text{corr}}(Z) = 1/(1 - Z Z_{\text{CM}})$ , where  $Z_{\text{CM}}$  denotes the point on the line of measurement at which both subcells are current matched. Moreover, the resulting correction is usually smaller than 1% (see also Table 1).

For spectrometric characterization, the following equation system is solved for different values of  $Z$ :

$$A_1 \int s_{\text{top}}(\lambda) e_1(\lambda) d\lambda + A_2 \int s_{\text{top}}(\lambda) e_2(\lambda) d\lambda = (1 + Z) \int s_{\text{top}}(\lambda) E_{\text{ref}}(\lambda) d\lambda \quad (15)$$

$$A_1 \int s_{\text{bot}}(\lambda) e_1(\lambda) d\lambda + A_2 \int s_{\text{bot}}(\lambda) e_2(\lambda) d\lambda = (1 - Z) \int s_{\text{bot}}(\lambda) E_{\text{ref}}(\lambda) d\lambda \quad (16)$$

For these values the light sources can then be adjusted and  $I$ - $V$  curves can be measured. Finally, the  $I$ - $V$  parameters are plotted against the normalized effective irradiance on the subcells. Figure 4 shows the spectrometric characterization of a  $\text{Ga}_{0.51}\text{In}_{0.49}\text{P}/\text{GaAs}$  dual-junction cell (cell 1) with AM1.5 global as reference spectrum. Each vertical set of  $I$ - $V$  parameters corresponds to one characteristic curve. Points are marked where the current mismatch is equivalent to AM0 or AM1.5 direct. The position and total irradiance of these points can be calculated by intersecting the line of measurement with the line through the origin and the respective standard spectrum (see Figure 3). Along the line of measurement the  $J_{\text{SC}}$  reaches a maximum when the subcells are current matched. As the effective irradiance on the top cell increases towards the right-hand side, spectra may be called 'blue-rich' on the right of the maximum and 'red-rich' on the left. From the spectrometric characterization graph, it is easy to determine at which point the dual-junction cell is current matched, not only in regard to the short-circuit condition, but also at the maximum power point.

Figure 4 also shows the calculated behavior of a dual-junction cell due to variation of the photocurrents of the subcells, using the equivalent circuit shown in Figure 1. The model parameters were taken from dark  $I$ - $V$  curves

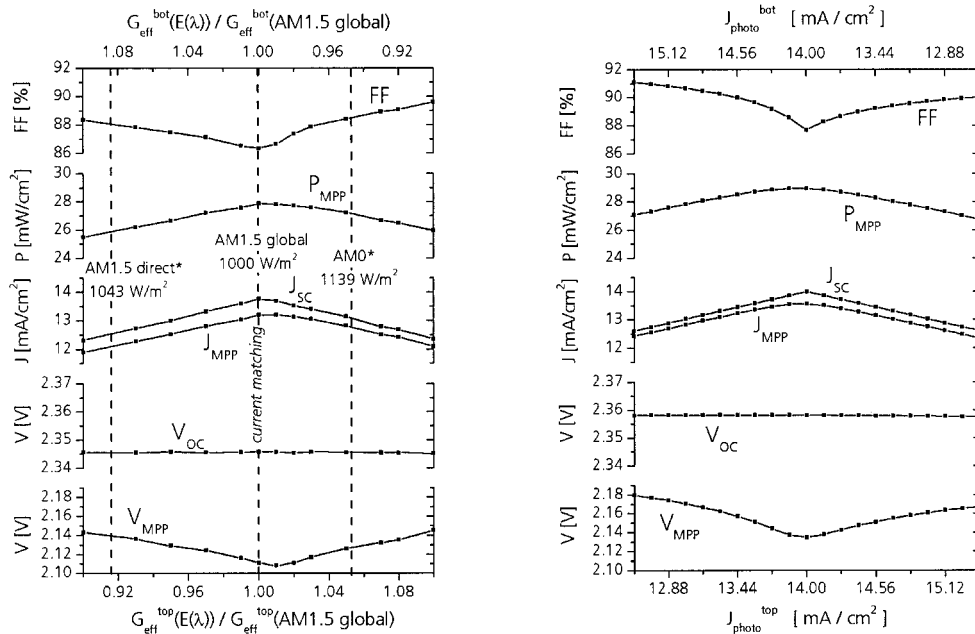


Figure 4. Spectrometric characterization of a  $\text{Ga}_{0.51}\text{In}_{0.49}\text{P}/\text{GaAs}$  dual-junction cell (cell 1) with AM1.5 global as reference spectrum (left) and calculated behavior of a dual-junction cell due to current mismatch (right)

of single-junction  $\text{Ga}_{0.51}\text{In}_{0.49}\text{P}$  and GaAs cells grown by MOVPE at Fraunhofer ISE. Spectrometric characterization and the calculation show the same characteristic behavior of the  $I$ - $V$  parameters.

The behavior of the  $J_{\text{SC}}$  shows the effect of current limitation. On the left of the graph, the top cell is limiting the current of the MJ cell. Moving to the right, the  $J_{\text{SC}}$  increases proportionally to  $G_{\text{eff}}^{\text{top}}$  until a maximum is reached. Since in Figure 4 this 'current-matching point' is located at AM1.5 global, cell 1 is current matched for this spectrum. Moving further to the right, the bottom cell becomes current limiting and the  $J_{\text{SC}}$  decreases proportionally to  $G_{\text{eff}}^{\text{bot}}$ . In principle, the  $J_{\text{MPP}}$  behaves similarly to the  $J_{\text{SC}}$ . However, the current-matching point for the  $J_{\text{MPP}}$  can differ from that for  $J_{\text{SC}}$ , especially if one subcell is shunted (see Figure 6).

The behavior of the  $V_{\text{MPP}}$  shows the shifting of the operating voltage. The  $V_{\text{MPP}}$  assumes a minimum at the current-matching point for the  $J_{\text{MPP}}$ , there being approximately equal to the sum of the  $V_{\text{MPP}}$  values of the subcells. The more the subcells are current mismatched, the more the operating voltage of the non-limiting subcell is shifted towards its  $V_{\text{OC}}$ . Therefore, as the current mismatch increases, so does the  $V_{\text{MPP}}$  of the MJ cell, approaching as a limit the sum of the  $V_{\text{MPP}}$  of the limiting and the  $V_{\text{OC}}$  of the non-limiting subcell.

In terms of accuracy of measurement there is hardly any dependence of the  $V_{\text{OC}}$  in the denoted range of spectral variation. If the  $J_{\text{MPP}}$  and  $J_{\text{SC}}$  behave similarly and  $V_{\text{OC}}$  stays constant, the fill factor (FF) shows a behavior analogous to the  $V_{\text{MPP}}$ . However, if the current-matching point of the  $J_{\text{MPP}}$  differs from that of  $J_{\text{SC}}$  due to one subcell being shunted, a totally different behavior of the FF can be observed (see Figure 6).

The  $P_{\text{MPP}}$  shows a much flatter maximum behavior than the  $J_{\text{MPP}}$  and the  $J_{\text{SC}}$  due to the minimum behavior of the  $V_{\text{MPP}}$  and the FF, respectively. It is important to note, that this general behavior is relevant for the performance of MJ concentrator cells under outdoor conditions. The power output is not as sensitive to the changes of the sun spectrum, as one would assume just considering losses from current limitation.

In this section, spectral metric and spectrometric characterization have been discussed for dual-junction cells only. In principle, procedures for more junctions can be derived by analogy. In the spectral metric for a triple cell, each spectrum can be identified by a point  $(G_{\text{eff}}^{\text{top}}, G_{\text{eff}}^{\text{mid}}, G_{\text{eff}}^{\text{bot}}) \in \mathbb{R}_+^3$ . The effect of current mismatch can be investigated on a 'plane of measurement', for which the sum of the effective irradiances on the subcells is constant. It is noteworthy, that the typical  $\text{Ga}_{0.51}\text{In}_{0.49}\text{P}/\text{GaAs}/\text{Ge}$  triple solar cell can be treated similarly to a  $\text{Ga}_{0.51}\text{In}_{0.49}\text{P}/\text{GaAs}$  dual-junction, if the Ge subcell has a very large excess current and therefore acts only as a 'voltage booster'.

## APPLICATIONS OF SPECTROMETRIC CHARACTERIZATION

One benefit from spectrometric characterization is that the absolute spectral response of the subcells can be calculated. At the current-matching point for the short-circuit condition  $(1 + Z_{\text{CM}}, 1 - Z_{\text{CM}})$ , the photocurrent of both subcells is equal to the measured value. The photocurrent density under the reference spectrum is equal to the measured peak  $J_{\text{SC}}$  value divided by  $(1 + Z_{\text{CM}})$  for the top and by  $(1 - Z_{\text{CM}})$  for the bottom cell. The absolute spectral response can then be calculated by scaling the relative spectral response to yield the correct  $J_{\text{SC}}$ , just as for single-junction cells.

Spectrometric characterization is very valuable for researchers who are testing new material systems and structures for MJ cells in order to compare them with well-developed structures, such as the  $\text{Ga}_{0.51}\text{In}_{0.49}\text{P}/\text{GaAs}$  dual-junction cell. Figure 5 shows the spectrometric characterization of a  $\text{Ga}_{0.51}\text{In}_{0.49}\text{P}/\text{Ga}_{0.95}\text{In}_{0.05}\text{As}$  (cell 2) and a  $\text{Ga}_{0.35}\text{In}_{0.65}\text{P}/\text{Ga}_{0.83}\text{In}_{0.17}\text{As}$  dual-junction cell (cell 3) manufactured at Fraunhofer ISE,<sup>19–21</sup> which are to be compared with a  $\text{Ga}_{0.51}\text{In}_{0.49}\text{P}/\text{GaAs}$  cell (cell 1, see Figure 4): If the cells were evaluated according to their efficiency at AM1.5 global, cell 1 would be the best. This is due to the fact that this cell is current matched for AM1.5 global, while the others are not. As mentioned earlier, the changing of the photocurrents of the subcells by varying the incident spectrum along the line of measurement corresponds to the changing of the photocurrents by varying the thickness of the top cell base layer. Therefore, the peak efficiency observed in the spectrometric characterization can be used as an approximation of the efficiency that could be reached if the cell design were adapted such that the dual-junction cell is current matched. It is noteworthy that this is just an approximation, since the voltage and also the optical properties of the dual-junction cell might change, if the thickness of the top cell base layer were modified.



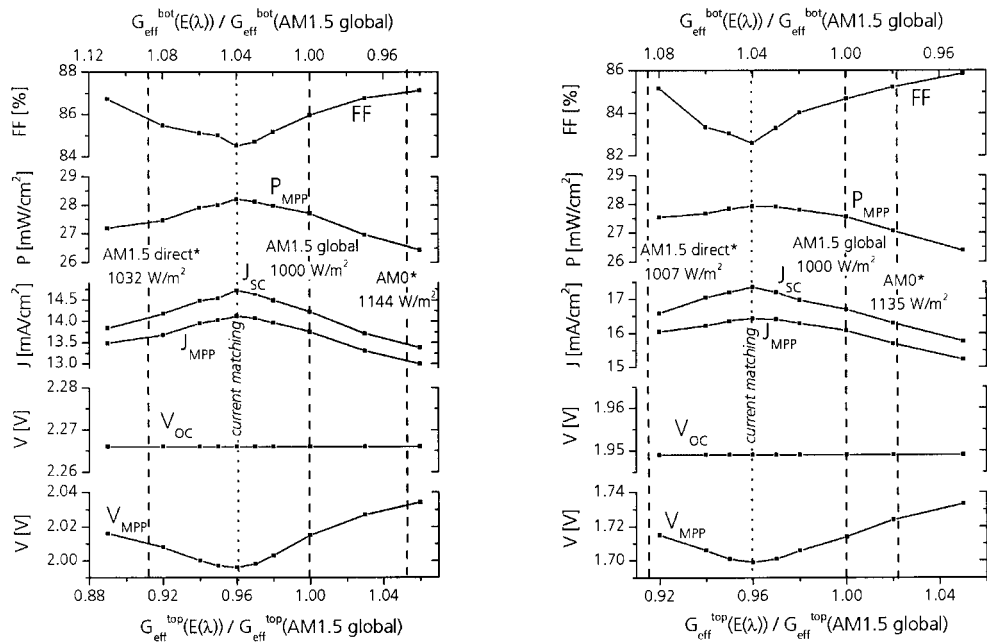


Figure 5. Spectrometric characterization of a  $\text{Ga}_{0.51}\text{In}_{0.49}\text{P}/\text{Ga}_{0.95}\text{In}_{0.05}\text{As}$  (cell 2, left) and a  $\text{Ga}_{0.35}\text{In}_{0.65}\text{P}/\text{Ga}_{0.83}\text{In}_{0.17}\text{As}$  dual-junction cell (cell 3, right)

However, new cell technologies can thereby be compared with state-of-the-art solar cells without the effort of current matching the cells to a reference spectrum in advance. With respect to the peak efficiency, cell 2 shows the largest potential for AM1.5 global (see Table I).

Depending on the application, in space or in terrestrial concentrator systems, the performance under AM0 or AM1.5 direct is important. In general it is best to perform spectrometric characterization with reference to the spectrum for which the comparison of the cells is intended. Anyhow, in the given example it is also possible to compare the cells with regard to AM0 or AM1.5 direct, using the calculated irradiances at the intersection points AM0\* and AM1.5 direct\* (see Figure 3). By calculating the respective peak efficiencies, it is shown that, for AM0, cells 2 and 3 show a high potential, while, for AM1.5 direct, cell 3 is the best choice. This result supports theoretical calculations, indicating that the material combination of cell 2 is well suited for AM0, as well as the material combination of cell 3 for AM1.5 direct.<sup>21</sup>

Table I. Comparison of three dual-junction cells of different material combination by spectrometric characterization with respect to the three standard spectra, AM1.5 global, AM0 and AM1.5 direct. The power and the irradiance of cells 2 and 3 were corrected to that on the 'ideal line' (Equation 13); the corrections applied were less than 0.4%

| Cell   | 1  | 2  | 3  |
|--|--|--|--|
| Material   | $\text{Ga}_{0.51}\text{In}_{0.49}\text{P}/\text{GaAs}$ | $\text{Ga}_{0.51}\text{In}_{0.49}\text{P}/\text{Ga}_{0.95}\text{In}_{0.05}\text{As}$ | $\text{Ga}_{0.35}\text{In}_{0.65}\text{P}/\text{Ga}_{0.83}\text{In}_{0.17}\text{As}$ |
| $\eta(\text{AM1.5 global}) (\%)$                 | 27.9   | 27.7   | 27.6   |
| $\eta_{\text{peak}}(\text{AM1.5 global}) (\%)$   | 27.9   | 28.3   | 28.0   |
| $G(\text{AM0}^*) (\text{W/m}^2)$                 | 1139   | 1142   | 1134   |
| $\eta_{\text{peak}}(\text{AM0}^*) (\%)$          | 24.5   | 24.8   | 24.7   |
| $G(\text{AM1.5 direct}^*) (\text{W/m}^2)$        | 1043   | 1036   | 1010   |
| $\eta_{\text{peak}}(\text{AM1.5 direct}^*) (\%)$ | 26.7   | 27.3   | 27.7   |

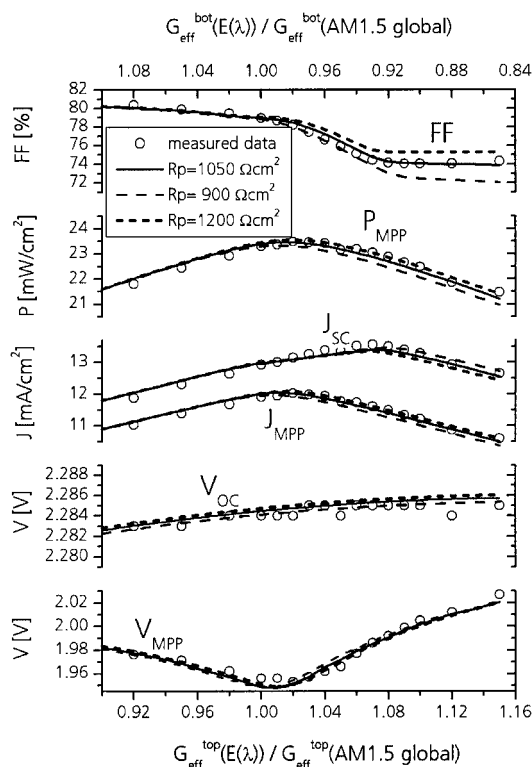


Figure 6. Spectrometric characterization of a  $\text{Ga}_{0.51}\text{In}_{0.49}\text{P}/\text{GaAs}$  dual-junction cell with a shunted bottom cell and calculated behavior for different shunt resistances  $R_p$  of the bottom cell

It is well known, that the light  $I$ - $V$  curve of a dual-junction cell reflects the shape of the current-limiting subcell.<sup>10,11</sup> Therefore, spectrometric characterization can be applied to estimate the properties of the different subcells. In Figure 6 the spectrometric characterization of a  $\text{Ga}_{0.51}\text{In}_{0.49}\text{P}/\text{GaAs}$  dual-junction cell is plotted, showing a typical behavior for the case that the bottom cell has a low shunt resistance, which is indicated by the large difference between  $J_{\text{MPP}}$  and  $J_{\text{SC}}$  for blue-rich spectra. It is important to note that, in this case, the FF has no local minimum. To estimate this low shunt resistance, the  $I$ - $V$  parameters were calculated for varying photocurrents, as shown in Figure 4, using the equivalent circuit of Figure 1. The model parameters were varied to resemble the behavior of the  $I$ - $V$  parameters observed in the spectrometric measurement. Especially, the fill factor showed a strong dependence on the shunt resistance of the bottom cell (Figure 6), which was determined to be  $1050 \pm 150 \Omega \text{ cm}^2$ . With regard to the other model parameters, it is not yet clear how well they can be estimated. Anyhow, from these model parameters the  $I$ - $V$  characteristics of the individual subcells can well be approximated, which yields valuable information for the optimization of the MJ cell.

This analytical method might also be valuable for the determination of the radiation response of the subcells of MJ space solar cells. Spectrometric characterization could be recorded after irradiating the MJ cell with different fluences of high energy protons and electrons. Existing evaluation methods for single-junction cells<sup>22</sup> could be applied, using the approximated  $I$ - $V$  characteristics of the individual subcells.

MJ cells are expected to be used in terrestrial high-concentration photovoltaic systems. One disadvantage of monolithic MJ cells is the loss of power due to the changes of the direct solar spectrum during periods of a day or year. Simulations proved that monolithic MJ cells still outperform single-junction cells despite these losses.<sup>3</sup> From spectrometric characterization it can be observed that the efficiency of MJ concentrator cells is not as sensitive to the changes of the incident spectrum as the current, because the increase of the fill factor partially compensates losses due to current mismatch. The question remains, how the annual power output of MJ concentrator cells at a specific site can be predicted. One reasonable approach is to define realistic reporting

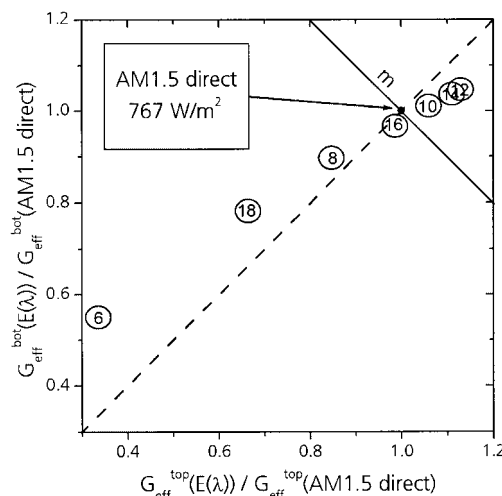


Figure 7. Change of the direct solar spectrum during the period of a day (Freiburg, midsummer) due to variation of air mass shown in the spectral metric of a  $\text{Ga}_{0.35}\text{In}_{0.65}\text{P}/\text{Ga}_{0.83}\text{In}_{0.17}\text{As}$  dual-junction cell. The plotted numbers indicate the time of day (summertime CET, GMT + 2)

conditions for MJ concentrator cells by a set of standard days.<sup>23,24</sup> Following this approach, the specific site can be described by an ensemble of different standard days. The definition of the standard days needs to include specifications on the changes of the direct solar spectrum during the day. Since spectrometric characterization describes the performance of the MJ cell under different spectral conditions, it can be used to calculate the power output of such a standard day. For illustration, spectra at different times of the day (Freiburg, midsummer) were simulated by SMARTS2<sup>25</sup> and plotted in the spectral metric of a  $\text{Ga}_{0.35}\text{In}_{0.65}\text{P}/\text{Ga}_{0.83}\text{In}_{0.17}\text{As}$  dual-junction cell (Figure 7).

Therefore, spectrometric characterization can be used to predict the performance of MJ concentrator cells under realistic conditions, eventually leading to an estimation of the annual energy output of photovoltaic concentrator systems.

## SUMMARY

Mathematical procedures have been presented which enable a faster way of spectral correction for multi-junction (MJ) solar cells compared with the commonly used calculation of the mismatch factor for each junction. The described procedure requires a multi-source simulator set-up, which allows variation of the intensity of the individual light sources without changing their spectral distribution. By this method the simulator spectrum can quickly be set to match the reference spectrum, significantly reducing the time required for calibration. These procedures also enable a systematic investigation of the behavior of the  $I$ – $V$  parameters of a MJ solar cell to variation of the incident spectrum.

A ‘spectral metric’ was introduced in analogy to colorimetry, in order to define scalar quantities (‘effective irradiance’) representing the spectrum. The measurement of the  $I$ – $V$  characteristics for different spectra is called ‘spectrometric characterization’, and points out the effects of current limitation and shifting of the operating voltage of the individual subcells. This analysis method yields information about the current matching of the subcells with higher reliability than measurement of the absolute spectral response. Using spectrometric characterization, the absolute spectral response of the subcells can be calculated from the measured relative spectral response. Information about the current matching at the maximum power point is given as well. From the observed peak efficiencies, different MJ cells can be compared without having to match the current of the structures for a reference spectrum in advance.

In addition, the properties of the individual subcells can be observed in the spectrometric characterization. By fitting the mathematical model of a series connection of two two-diode models, including shunt and series resistance, to the spectrometric measurement, the diode parameters can be estimated. These can be used to calculate the  $I$ - $V$  characteristics of the individual subcells, yielding valuable information for the optimization of the MJ cell. This analytical method might also be valuable for the determination of the radiation response of the subcells of MJ space solar cells. Existing evaluation methods for single-junction cells can be applied, using the approximated  $I$ - $V$  characteristics of the individual subcells.

Since spectrometric characterization describes the performance of the MJ cell under different spectra, it can be used to estimate the changing performance of MJ concentrator cells over the period of a day. By defining a year at a specific site as a set of standard days, the annual power output of the MJ cell can be estimated from spectrometric characterization recorded under concentration. Therefore, spectrometric characterization is a powerful analytical tool, not only for the optimization, but also for the prediction of the realistic performance of MJ solar cells

### Acknowledgements

The authors wish to thank Keith Emery from the National Renewable Energy Laboratory (NREL) in Golden, Colorado, and Rob Walters from the US Naval Research Laboratory (NRL) in Washington DC for valuable discussions. Further, they wish to thank Rolf Beckert, Elisabeth Schäffer, Ute Schubert, Carsten Baur, Tom Tibbits and Gerald Siefer at Fraunhofer ISE for technical support. J. Bartlau, K. Bücher, K. Heidler, G. Kleiss, B. Müller-Bierl and A. Schoenecker are acknowledged for earlier work. This work was supported by the German Ministry of Economy and Technology (BMWi) under contract number 0328554E. The authors are responsible for the contents.

### REFERENCES

1. Green MA, Emery K, King DL, Igari S, Warta W. Solar cell efficiency tables (version 18). *Progress in Photovoltaics: Research and Applications* 2001; **9**: 287–293.
2. Emery K, Osterwald CR, Glatfelter T, Burdick J, Virshup G. A comparison of the errors in determining the conversion efficiency of multijunction solar cells by various methods. *Solar Cells* 1988; **24**: 371–380.
3. Faine P, Kurtz SR, Riordan C, Olson JM. The influence of spectral solar irradiance variations on the performance of selected single-junction and multijunction solar cells. *Solar Cells* 1991; **31**: 259–278.
4. Glatfelter T, Burdick J. A method for determining the conversion efficiency of multiple-cell photovoltaic devices. *Proceedings of the 19th IEEE Photovoltaic Specialists Conference*, New Orleans, 1987; 1187–1193.
5. Heidler K, Müller-Bierl B. Measurement of multijunction solar cells. *Proceedings of the 22nd IEEE Photovoltaic Specialists Conference*, Las Vegas, 1991; 430–435.
6. Virshup GF. Measurement techniques for multijunction solar cells. *Proceedings of the 21st IEEE Photovoltaic Specialists Conference*, Kissimmee, 1990; 1249–1255.
7. Nagamine F, Shimakawa R, Suzuki M, Abe T. New solar simulator for multi-junction solar cell measurements. *Proceedings of the 23rd IEEE Photovoltaic Specialists Conference*, Louisville, 1993; 686–690.
8. Emery K, Osterwald CR, Cannon TW, Myers DR, Burdick J, Glatfelter T, Czubytyj W, Yang J. Methods for measuring solar cell efficiency independent of reference cell or light source. *Proceedings of the 18th IEEE Photovoltaic Specialists Conference*, Las Vegas, 1985; 623–628.
9. Adelhelm R, Buecher K. Performance and parameter analysis of tandem solar cells using measurements at multiple spectral conditions. *Solar Energy Materials and Solar Cells* 1988; **50**: 185–195.
10. Burdick J, Glatfelter T. Spectral response and  $I$ - $V$  measurements of tandem amorphous-silicon alloy solar cells. *Solar Cells* 1986; **18**: 301–314.
11. Kurtz SR, Emery K, Olson JM. Methods for analysis of two-junction, two-terminal photovoltaic devices. *Proceedings of the 1st World Conference on Photovoltaic Energy Conversion*, Waikoloa, Hawaii, 1994; 1733–1737.
12. King DL, Hansen BR, Moore JM, Aiken DJ. New methods for measuring performance of monolithic multi-junction solar cells. *Proceedings of the 28th IEEE Photovoltaic Specialists Conference*, Anchorage, 2000; 1197–1201.

13. ASTM E44 Draft 200R10. *Standard Test Method for Measurement of Electrical Performance and Spectral Response of Nonconcentrator Multijunction Photovoltaic Cells and Modules*, October 2000.
14. Emery K, Meusel M, Beckert R, Dimroth F, Bett A, Warta W. Procedures for evaluating multijunction concentrators. *Proceedings of the 28th IEEE Photovoltaic Specialists Conference*, Anchorage, 2000; 1126–1130.
15. Field H, Emery KA. An uncertainty analysis of the spectral correction factor. *Proceedings of the 23rd IEEE Photovoltaic Specialists Conference*, Louisville, 1993; 1180–1187.
16. Bartlau J, Adelhelm R, Bücher K. Measurement of the efficiency (power) temperature coefficient of tandem solar cells. *Proceedings of the 2nd World Conference on Photovoltaic Solar Energy Conversion*, Vienna, 1998; 3646–3649.
17. Hardy AH. The physical basis of color specification. *Handbook of Colorimetry*. Cambridge, Massachusetts, 1936. ISBN 026208001X.
18. Adelhelm R, La Roche G. Matching of multi-junction solar cells for solar array production. *Proceedings of the 28th IEEE Photovoltaic Specialists Conference*, Anchorage, 2000; 1336–1339.
19. Dimroth F, Lanyi P, Meusel M, Schubert U, Bett AW. New lattice mismatched GaInP/GaInAs tandem solar cell concepts for high efficiency space and terrestrial concentrator solar cells. *Proceedings of the 16th European Photovoltaic Solar Energy Conference*, Glasgow, 2000; 106–109.
20. Dimroth F, Sulima OV, Bett AW. Recent progress in the development of III-V solar and thermophotovoltaic cells. *Compound Semiconductors* 2000; **6**: 53–57.
21. Dimroth F, Beckert R, Meusel M, Schubert U, Bett AW. Metamorphic GaInP/GaInAs tandem solar cells for space and for terrestrial concentrator applications at  $C > 1000$  suns. *Progress in Photovoltaics: Research and Applications* 2001; **9**: 165–178.
22. Messenger SR, Summers GP, Burke EA, Walters RJ, Xapsos MA. Modeling solar cell degradation in space: a comparison of the NRL displacement damage dose and the JPL equivalent fluence approaches. *Progress in Photovoltaics: Research and Applications* 2001; **9**: 103–121.
23. Kroposki B, Myers D, Emery K, Mrig L, Whitaker C, Newmiller J. Photovoltaic module energy rating methodology development. *Proceedings of the 25th IEEE Photovoltaic Specialists Conference*, Washington DC, 1996; 1311–1314.
24. Marion B, Kroposki B, Emery K, Myers delCueto J, Osterwald C. Validation of a photovoltaic module energy ratings procedure at NREL. *Technical Report NREL/TP-520-26909*, 1999.
25. Gueymard C. SMARTS2, a simple model of the atmospheric radiative transfer of sunshine: algorithms and performance assessment. *Report FSEC-PF-270-95*, 1995.